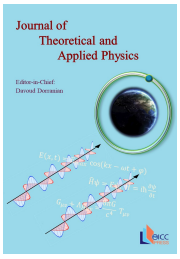

Volume 17, Issue 1, 172313 (1-9)

Journal of Theoretical and Applied Physics (JTAP)

https://dx.doi.org/10.57647/j.jtap.2023.1701.13

Numerical investigation of the fullerene and doped fullerene effects on thermal performance of water base-fluid

Ahmad Saadi [1], Hamid Reza Vanaie [2]*, Mojtaba Yaghobi [3], Ebrahim Heidari [2], Darush Masti [1]

[1] *Department of Nuclear Engineering, Bushehr Branch, Islamic Azad University, Bushehr, Iran.*
[2] *Department of Sciences, Bushehr Branch, Islamic Azad University, Bushehr, Iran.*
[3] *Department of Physics, Ayatollah Amole Branch, Islamic Azad University, Amol, Iran.*

***Corresponding author**: hamid.vanaie@hotmail.com

Received 19 July 2022; Accepted 7 December 2022; Published online 11 December 2022

Abstract:
In this study, the fullerenes have been inserted into water base-fluid to investigate the atomic and thermal behavior of nanofluid and hybridnanofluid as heat transfer fluid. This choice derives from low cast and high thermal stability of this nanostructure. Our computational results from Molecular Dynamics (MD) simulations indicate that the addition of nanoparticles with 4% atomic ratio produced an appreciable effect on the nanofluid. The maximum value of density, velocity, and temperature profile have reached to 0.029 atom/(cubicÅ), 0.005 $Å/ps$, and 321 ^oC. Its thermal conductivity would increase to 0.82 W/mK Heat flux reached to 2019 kW/m^2 after t= 10 ns. Also, the aggregation phenomenon detected after t= 5.84 ns. This hybridnanofluid has been used to enhance the energy efficiency of the heat exchangers at high temperature for the nuclear industry applications for the first time. Numerically, by the temperature increase of nanofluid structure to 625.15 K, thermal power of nanofluid reached to 3881 MW. The thermal performance of hybridnanofluid can be improved by more than 30% by adding concentration of fullerene and doped fullerene at 4 vol%.

Keywords: Heat transfer; Fullerene; Doped fullerene; Hybridnanofluids; Molecular dynamics

1. Introduction

Nanotechnology is the design, characterization, production, and application of structures, devices, and systems through controlled manipulation of size and shape at the atomic (nanometer) scale with the products exhibiting at least one novel/superior characteristic or property [1–3]. Nanofluids are the promising structures in nanotechnology area [4, 5]. In recent years, these nanostructures have been used commonly in mass and heat transfer phenomena for industrial applications [6–8]. Technically, nanofluids contain a small volume fraction of nanoparticles, nanowires, or nanotubes for targeted changes in thermal, rheological, and other properties [9, 10]. As reported in other works, the thermal behavior of various nanofluids makes them suitable for many industrial, medical, etc. applications. So the thermal behavior of these structures represents an important topic in today science.

Hybrid-nanofluids are potential fluids that present superior thermophysical properties and thermal performance than common heat transfer fluids mono-nanofluids. Hybrid nanofluid is a new fluid produced by dispersing two dissimilar types of nano-particles into the base fluid. Some researchers have reported that conventional coolants could be replaced by hybrid-nanofluids, particularly fluids that work at very high temperatures. Accordingly, these types of nanofluids could lead to saving energy [11–14]. For the atomic study of common nanofluids, various methods have been introduced by researchers. Molecular Dynamics (MD) approach is one of the best methods to describe the atomic and thermal behavior of nano-scale structures [15–18]. Previous research have reported the appropriate performance of MD simulations in thermal behavior of nanometric structures. Jolfaei et al. [19] calculated the thermal properties

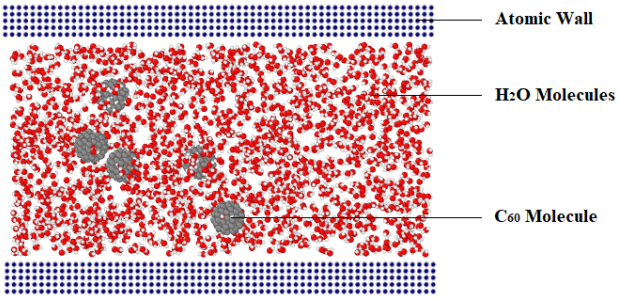

Figure 1. Schematic of H_2O-fullerene nanofluid inside atomic channel in initial time step of MD simulation.

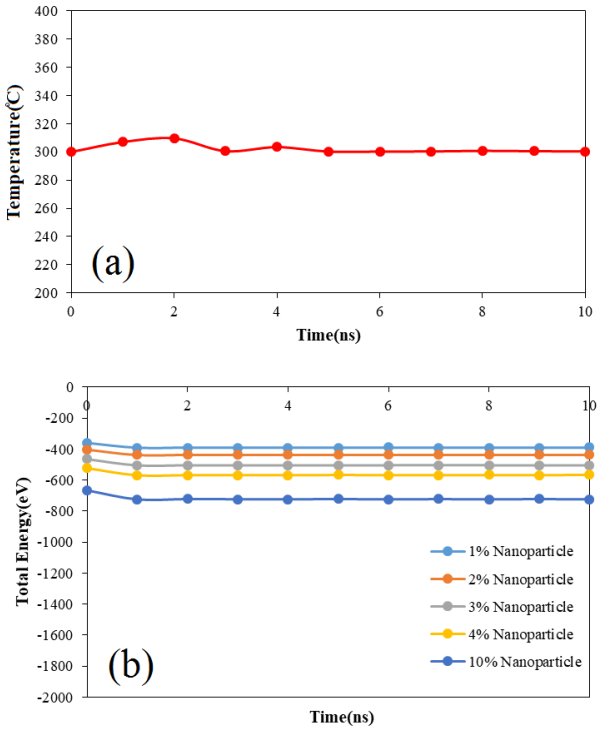

Figure 2. (a)Temperature, and (b)total energy variation of H_2O-fullerene nanofluid as a function of MD simulation time.

of deoxyribonucleic acid with precise atomic arrangement via equilibrium and non-equilibrium molecular dynamics approaches. In these methods, each deoxyribonucleic acid molecule is represented by C, N, O, and P atoms and is implemented dreiding potential to describe their atomic interactions. Their results showed the calculated rate of thermal conductivity via equilibrium and non-equilibrium molecular dynamics methods was 0.381 W/m K and 0.373 W/m K, respectively. By comparing results from these two methods, it was found that the results from equilibrium and non-equilibrium molecular dynamics methods were relatively identical. Asgari et al. [20] reported the atomic behavior of H_2O/Cu nanofluid by using MD simulation approach. The copper nanochannel with sphere barriers was simulated to study the nanofluid flow and the atomic interactions of these structures were described by embedded atom model and Lennard-Jones (LJ) interatomic potentials. Technically, to study the atomic behavior of these structures, physical parameters such as temperature, density and velocity profiles of the nanofluid were reported. MD results show that such parameters of H_2O/Cu nanofluid inside non-ideal nanochannel affected by atomic barriers' number and size of them changes. In other computational work, Ashkezari et al. [21] reported the thermal conductivity of Human serum albumin (HSA) with equilibrium/non-equilibrium molecular dynamic approaches. In these methods each HSA molecule is exactly represented by C, N, O and S atoms and their implemented dreiding potential. Finally by using Green-Kubo and Fourier's law the thermal conductivity of HSA/H_2O mixture was calculated. Their calculated values for thermal conductivity via equilibrium/non-equilibrium molecular dynamics methods were 0.496 W/m K and 0.448 W/m K, respectively. The calculated thermal conductivity of the understudy structure was very close to the thermal conductivity calculated for water molecules as reported by other research groups.

In this work, we used fullerenes nanoparticles with 1%, 2%, 3%, 5%, and 10% atomic ratio to improve the thermal behavior of H_2O molecules as base-fluid. In fullerene, carbon atoms are arranges in honeycomb structure with strong bonds, which makes them stable against high ratio of pressure and temperatures. On the other hand, the structural form of fullerene causes appropriate rotational and translational movements during heat transfer process. Therefore, this type of nanoparticle have been used in current research to improve heat transfer ratio inside base fluid for common applications in nuclear industries. Regarding the computational processes, an MD simulations tool of the type Large-scale Atomic/Molecular Massively Parallel Simulator (LAMMPS) manufactured by Sandia National Laboratories (2021) was used [22–24]. During the MD simulations, the ideal (atomically) fullerenes nanoparticles were inserted into initial water base-fluid inside atomic channel and the evolution of simulated structures were reported to design optimized atomic arrangement for various applications such as heat and mass transfer in industrial, medical and etc. applications.

2. Computational details

Technically, MD simulation is one of the promising methods to describe the atomic behavior of various nanostructures such as nanocomposites, nanofluids, etc. This computational approach is utilized in the present paper to describe the atomic/thermal behavior of H_2O base-fluid in the presence of fullerenes nanoparticles with various atomic ratios. The time evolution of H_2O-fullerene nanofluid was performed using Newton's equation, where the atomic interaction between various nanostructures is defined with the inter-atomic potential concept. H_2O molecules in current study was modeled by TIP4P model [25]. Here, the atomic interaction between H_2O molecules and fullerenes was determined by Universal Force Field (UFF) [26]. The Lennard-Jones (LJ) equation is implemented in this poten-

Table 1. Computational details in our MD simulations.

Simulation Parameter	Parameter Ratio/Setting
Box Length	$100 \times 65 \times 65\ \mathring{A}^3$
Boundary Condition in X, Y, and Z Directions	Periodic, Periodic, and Fix
Simulation Algurithms	NPT/NVE
Initial Temperature	321 ^{o}C
Initial Pressure	16 MPa
Time Step	1 fs
Temperature Damping Ratio	10
Pressure Damping Ratio	100

tial to describe the nonbond interactions [27]:

$$U(r_{ij}) = 4\varepsilon\left[\left(\frac{\sigma}{r_{ij}}\right)^{12} - \left(\frac{\sigma}{r_{ij}}\right)^{6}\right] \quad r_{ij} \leq r_c \tag{1}$$

where ε constant, σ constant, and r_{ij} represent the minimum potential's depth, the diameter of an atom, and the distance between various atoms (i and j), respectively. Furthermore, the simulated atomic walls as depicted in figure 1, denotes the interaction between nanofluid particles and LJ. Finally, fullerene nanoparticles were modeled by TERSOFF potential in MD simulation box [28, 29]. The following equation can describe the TERSOFF potential function:

$$E = \frac{1}{2}\Sigma_i\Sigma_{j\neq i} f_C(r_{ij})[f_R(r_{ij}) + b_{ij} f_A(r_{ij})] \tag{2}$$

where, f_R is a 2 body term and f_A includes 3 body interactions. After the interatomic potential was defined in the simulated structures, the MD approach steps were followed. For this purpose, the nanostructures were interacted and moved to other positions with new atomic velocity. The atomic force (F_i), position (r_i), and momentum (P_i) of atoms can be calculated by the following equations [30]:

$$F_i = m_i a_i = m_i \frac{d^2 r_i}{dt^2} \tag{3}$$

$$P_i = m_i v_i \tag{4}$$

In these formalisms, the interatomic potential functions relate to the calculated forces for each atom [30]. In the next step of MD simulations procedure, Nose-Hoover barostat implemented to atomic structures to set initial condition (temperature) in MD simulation box [31,32]. In this barostat the below equations was used for "F" physical parameter calculation [33]:

$$f(N.V.T) = [N!Q(N.V.T)]^{-1} \int dr^N$$

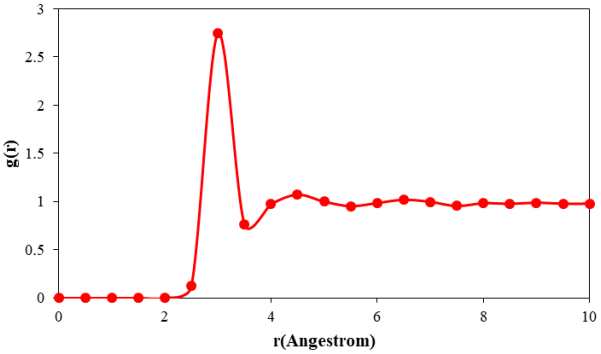

Figure 3. The O-O radial distribution function (RDF) after equilibrium process.

$$\times \int dp^N e^{\frac{-H_1(r^N.p^N.V)}{KT}} F(r^N.p^N.V) \tag{5}$$

where

$$Q(N.V.T) = (N!)^{-1} \int dr^N \int dp^N e^{\frac{-H_1(r^N.p^N.V)}{KT}} \tag{6}$$

where, N is the number of atoms, V is volume of structure, H is Hamiltonian, p is atomic momentum, p denoted the pressure, and K represents the Boltzmann constant. Finally, the Velocity-Verlet algorithm was used to associate the motion equations and time evolution of nanostructures which were estimated for the phase space calculation [34–37]. According to the above described details, the MD simulations in current work were carried out following the below two steps:

Step 1: H_2O-fullerene/fullerenes nanofluid/hybridnanofluid was simulated with TIP4P model, UFF and Tersoff potentials inside the atomic walls as shown in figure 1. In our defined samples periodic boundary condition implemented for X and Y directions and fix one used for Z direction. By using these boundary settings, the modeled sample continued to infinity in X and Y directions. As a result, MD outputs which obtained in current research can be considered in actual applications to improve the thermal behavior of the common fluids. Also, modeled compound was minimized geometrically through

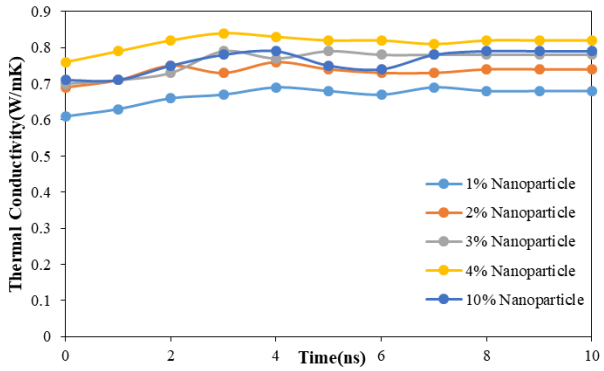

Figure 4. The thermal conductivity of H_2O-fullerene nanofluid variation as a function of nanoparticle ratio and MD simulation time.

Table 2. The thermal conductivity, aggregation time, and thermal power of H_2O-fullerene nanofluid/hybrid nanofluid as a function of nanoparticles atomic ratio.

Atomic Ratio of Fullerene Nanoparticles(%)	Thermal Conductivity (W/m.K)	Atomic Aggregation Time (ns)	Thermal Power (MW)
1	0.68/0.81	7.08	3122/3241
2	0.74/0.85	6.83	3208/3312
3	0.78/0.89	6.59	3459/3570
4	0.82/0.92	5.84	3881/3988
10	0.79/0.89	5.49	3661/3780

conjugate gradient method [38, 39]. Then, the minimized structure equilibrated by using NPT ensemble for t= 10 ns. For this purpose, initial value of atomic temperature was set at T_0 = 321 ^{o}C and P_0 = 16 MPa. in this step, the physical stability of H_2O-fullerene nanofluid was reported through the temperature and total energy calculation.

Step 2: Next, thermal evolution process was implemented to equilibrated H_2O-fullerene/fullerenes nanofluid/hybridnanofluid for t= 10 ns with NVE ensemble [40]. After this atomic evolution, some physical parameters such as: thermal conductivity, heat flux, thermal power, aggregation time, density, velocity, temperature profile, and effective voltage were reported to describe the thermal behavior of simulated nanofluid. Our computational settings in current research reported in Table 1.

3. Computational results

3.1 Physical stability of nanofluid/hybridnanofluid

In the first step of our computational study, the equilibrium phase of H_2O-fullerene nanofluid was reported to be at T_0 = 321 ^{o}C as initial temperature. Our results in this step show that the atomic position and defined interatomic potential in nanofluid arrangement are matched with each other properly. This result was described by temperature and total energy calculation after t= 10 ns (as shown in figure 2). Our MD calculations indicated that the temperature of atomic nanofluid was converged to 321 ^{o}C. This thermal behavior shows that t= 10 ns is a sufficient MD time for equilibrium phase detection. Also, total energy calculation would indicate the equilibrium phase of the simulated H_2O-fullerene nanofluid. As depicted in figure 2(b), the total energy of nanofluid would increase by fullerene atomic ratio enlarging in MD simulation box. Numerically, the nanoparticles' atomic ratio will increase from 1% to 10%, and the total energy of nanofluid will increase from -389.360 eV to -723.057 eV. The total energy enlargement by the insertion of fullerene nanoparticles to base-fluid shows an atomic stability and attraction force increase between various part of simulated structures. We expected the change of thermal behavior of H_2O base-fluid affected by nanoparticles' atomic ratio. Physically, attraction force between various atoms would cause the improvement of thermal behavior of pristine fluid (water molecules) which is described exactly in the next computational step.

Hybridnanofluid increase stability and improve of suspension of nano-particles by adding the type of doped fullerene. Next, to validate the computational method in the current simulations, the Radial distribution function (RDF) and the density of water are calculated. The RDF of simulated structures can describe the atomic arrangement of them. Computationally, the RDF denoted in equation (7) by $g(r)$, describes the probability of finding particles at r distance from other atoms [41],

$$g(r) = \frac{1}{4\pi\rho}\frac{dn_r}{dr} \tag{7}$$

where ρ is the atomic density, dn_r is a function that calculates the number of atoms within a shell of thickness dr.

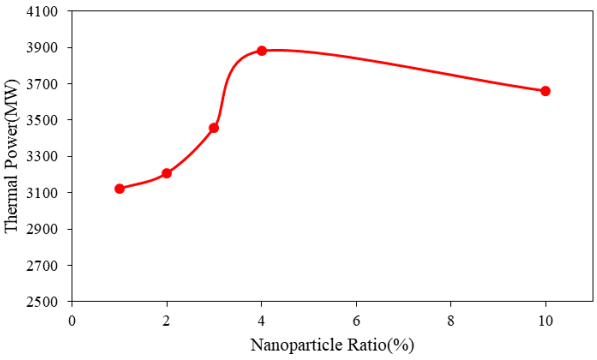

Figure 5. The thermal power of H_2O-fullerene nanofluid variation as a function of nanoparticle ratio.

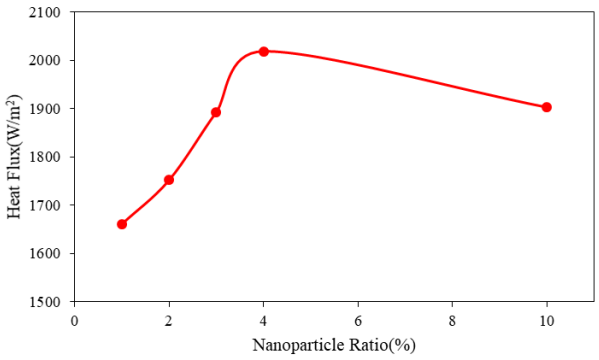

Figure 6. The heat flux of H_2O-fullerene nanofluid variation as a function of nanoparticle ratio.

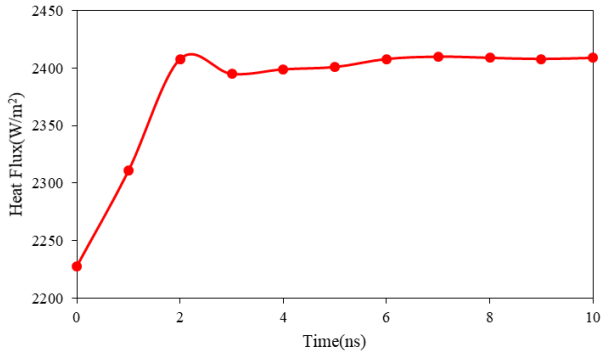

Figure 7. The thermal conductivity of H_2O-fullerene nanofluid at T_0= 625.15 ^{o}C variation as a function of MD simulation time.

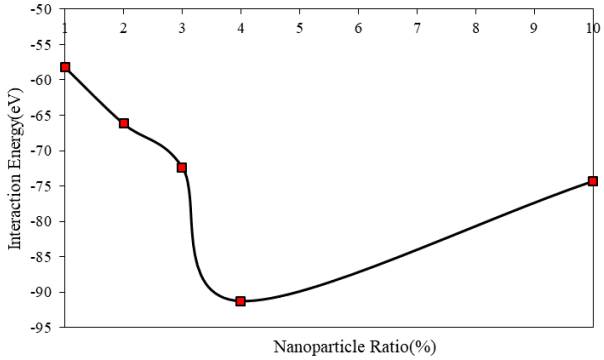

Figure 8. The interaction energy between various atoms as a function of nanoparticles inside MD box.

Figure 3 shows RDF of O atoms in H_2O molecules which is consistent with the previous reports [42].

3.2 Thermal behavior of H_2O-fullerene nanofluid

After the equilibrium phase of simulated structures, the thermal behavior of H_2O-fullerene/fullerenes nanofluid/hybridnanofluid was reported. In this step of our calculations, we use the Green-Kubo approach to describe the thermal behavior of simulated nanofluid [43–45]. Technically, thermal calculation in current study was done using micro-canonical ensemble (NVE) as equation:

$$k = \frac{1}{3k_B V T^2} \int_0^\infty < S(t).S(0) > dt \qquad (8)$$

In this equation k_B, V, and S define Boltzmann constant (1.380649×10^{-23} J.K^{-1}), volume, and the heat vector, respectively. At each simulation time step in LAMMPS computational package, the heat current of atoms can be estimated using velocity and stress tensor. The mean of the heat current autocorrelation function is represented by $< S(t).S(0) >$. Figure 4 shows the thermal conductivity ratio vs. fullerene atomic ratio in MD simulation box. As depicted in this figure, the thermal conductivity of H_2O-fullerene nanofluid reach to the final ratio after t= 10 ns. The results listed in Table 2 were averaged over the simulation box directions to get the accurate ratio. The calculated results show that the fullerene and doped fullerene with 4% atomic ratio effectively improve the thermal behavior of H_2O molecules, resulting from a large contact surface between the fullerene nanoparticle and base-fluid atoms. This procedure detected in previous researches and verified our computational technique in current research [37,46–48]. Nonoparticles aggregation process in nanofluid structures is an important parameter for heat and mass transfer process. Physically, by fullerene nanoparticles insertion to H_2O base fluid with high atomic ratio, the atomic mobility of nanostructures would increase and the aggregation process is detected in shorter MD time. As reported in Table 2, by the use of nanoparticles in MD box with 4% atomic ratio, the contact surface between various nanoparticles was decreased and the aggregation process was detected after t= 5.32 ns. Through this mechanism, the energy transition rate in simulated structure was enlarged and finally the MD time for various physical phenomenon such as heat and mass transfer was decreased. By estimating thermal power of simulated nanofluid inside the nanostructures (nanochannels), one can estimate these atomic structures' behavior as cooling systems in various actual applications such as nuclear engineering-based systems. The thermal power is another important parameter which can be described via thermal behavior of simulated structures. Thermal power of the fuel rods is determined with the help of power peaking factors presented [49–51].

Table 3. The heat flux of H_2O-fullerene nanofluid as a function of nanoparticles atomic ratio.

Atomic Ratio of Fullerene Nanoparticles (%)	Heat Flux (W/m^2)
1	1661
2	1752
3	1893
4	2019
10	1903

The MD outputs indicated that by nanoparticles adding to pristine fluid, the thermal power of atomic structure was increased. The use of 4% fullerene nanoparticles inside MD box caused an increase of total system thermal power from 3000 to 3881 MW. Physically, phonon vibration increasing inside pristine fluid by adding nanoparticles to them cause heat flux ratio which transferred inside MD box increased and thermal conductivity of modeled nanofluid improved. The computational results indicated that water-fullerene nanofluid can be used in coolant systems in the nuclear engineer industry. Furthermore, simulation results indicated by using nanoparticles with more than 4% ratio, some inappropriate phenomenon such as aggregation of nanoparticles occur in lesser simulation time and thermal efficiency of modeled samples decreased. In another modeled sample in current computational research, by adding nanoparticles with 20% ratio, thermal conductivity dropped to 0.73 W/m.K.

Also, coolants could be replaced by hybrid-nanofluids, par-

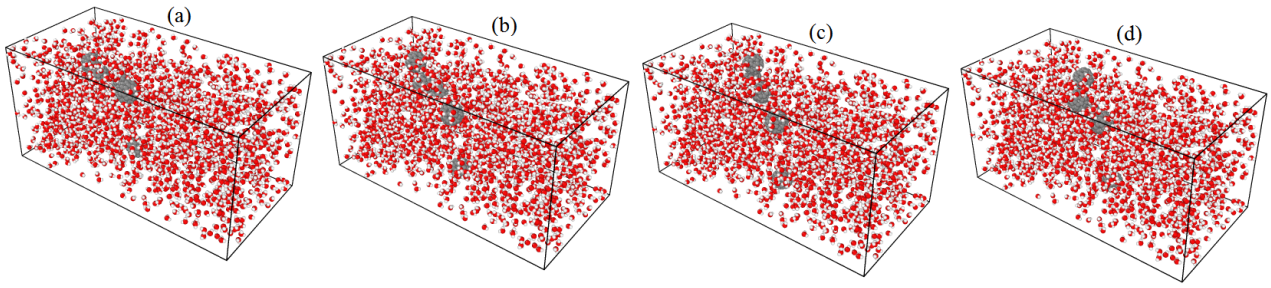

Figure 9. Atomic evolution of H_2O-fullerene nanofluid at: (a) t= 0 ns, (b) t= 2 ns, (c) t= 5ns, and (d) t= 10 ns

ticularly fluids that work at very high temperatures. Our results show that thermal-conductivity in hybridnanofluid increases and improve heat transfer performance (Table 2). Figure 5 illustrates the thermal power variation of simulated systems as a function of nanoparticles ratio. As can be seen in this figure, by nanoparticles addition to base fluid by >4% atomic ratio, the thermal power of simulated structures was decreased. This decrease arises from the nanoparticles aggregation process.

Thermal behavior improvement of simulated nanofluid by the increase of nanoparticles ratio can be effected via the heat flux ratio calculation. Figure 6 represents this parameter variation as a function of nanoparticle ratio and MD time. By adding greater amount of fullerene nanoparticles to base fluid, the ratio atoms' mobility would increases. So, more thermal energy and heat flux would flow inside the MD box. Numerically, by an increase of 1 to 5% ratio of fullerene nanoparticles, the net heat flux would vary from 1661 W/m^2 to 2019 W/m^2, respectively (as shown in Table 3 and figure 7). The temperature variation of simulated structures cause thermal behavior variations in them. For this purpose, the temperature of simulated nanofluid in presence of 1% nanoparticle was set to 352 ^{o}C. The ratios and thermal conductivity of final atomic structures have been reported in this section. This ratio is the operating temperature of common reactors in the nuclear engineering industry systems. By initial temperature increasing in atomic nanofluid, the fluctuations' amplitude would increase against higher temperature. This atomic procedure would cause heat flux increasing inside the MD box. After equilibration phase of nanofluid detection at T_0= 352 ^{o}C, the heat flux which flows in atomic nanofluid would reach to 2405 KW/m^2. This heat flux increase in simulated models, the thermal conductivity of pristine atomic systems would reach to larger ratios and would converge to 4003 W/m.K. Computationally, the heat flux in the current study was calculated by using Green-Kubo method.

To more analayzing of thermal conductivity in defined nano-fluid, interaction energy inside MD box calculated in this step. As shown in figure 8, by nanoparticle ratio enlarging to 4%, interation energy inside MD box reached to -91.25 eV. By more nanoparticles ratio increasing, interatomic distance inside box decreases and replusive force between them convergd ti higher value. Numerically, by nanoparticle ratio setting to 10%, interaction energy converged to -74.31 eV. Structurally, figures 9 indicated the atomic position of atoms in as a function of MD time. As shown in this figure various parts, nanoparticles don't aggregated before t= 5 ns. This time evolution indicated appropriate behavior of fullerene nanoparticles as thermal improved parameter for heat transfer applications at high temperature and pressure condition.

The atomic evolution of H_2O-fullerene nanofluid is defined by their density, velocity, and temperature profiles inside the atomic channel. For this calculation, the simulation box is divided into 122 bins in z direction. The calculated results show that the density profile of H_2O-fullerene nanofluid converge a maximum ratio at initial and final bins. Numerically, the maximum value of the density profile changes from 0.019 atom/$\AA^3$ to 0.032 atom/$\AA^3$ values by 1% to 10% nanoparticles adding to water base-fluid, respectively (as depicted in figure 10). This atomic behavior arises from

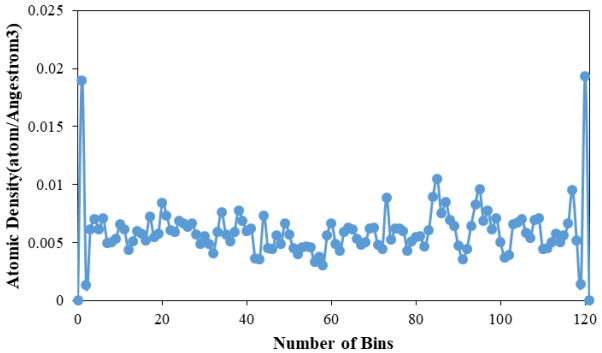

Figure 10. Density profile of H_2O-fullerene nanofluid with 4% nanoparticle in MD simulation box after t= 10 ns.

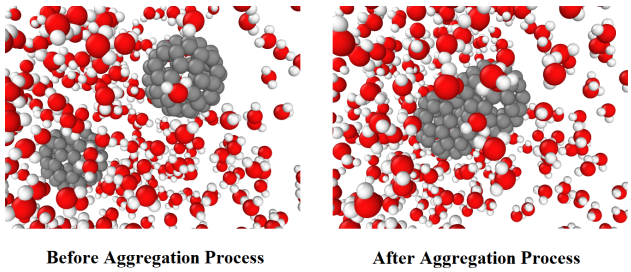

Figure 11. Atomic arrangement of H_2O and fullerene molecules, before and after of aggregation process.

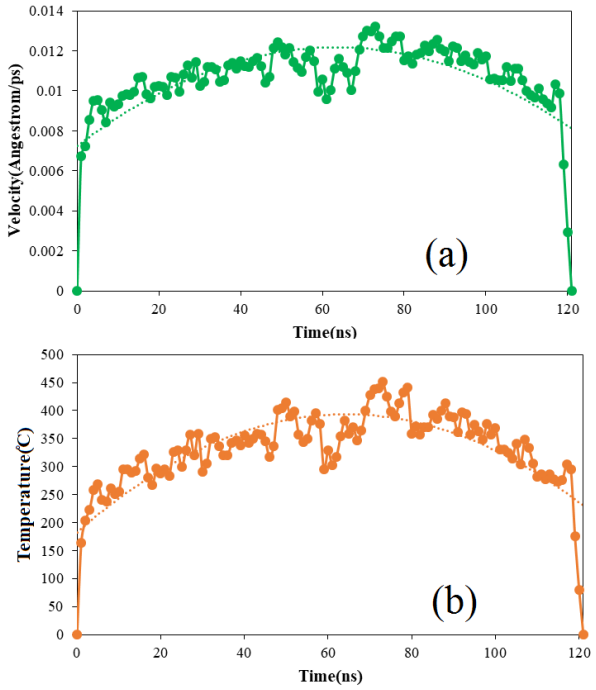

Figure 12. (a) Velocity and (b)temperature profile of H_2O-fullerene nanofluid with 4% nanoparticle in MD simulation box after t= 10 ns.

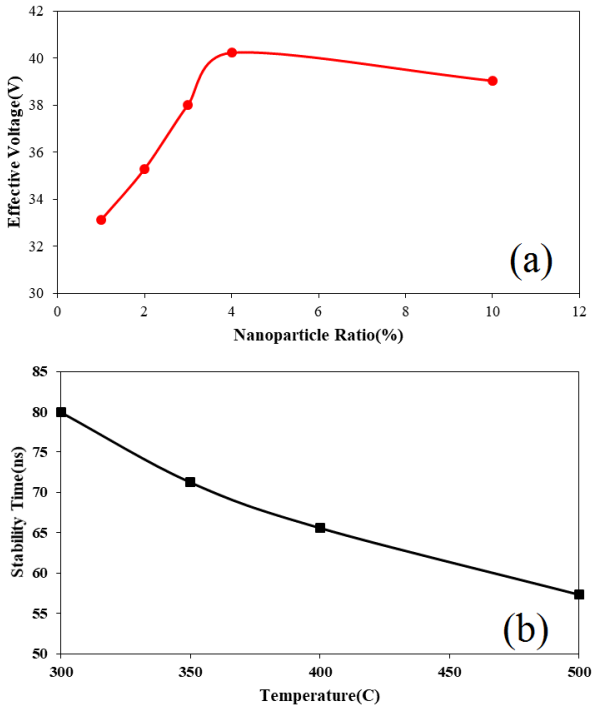

Figure 13. (a) The effective voltage of H_2O-fullerene nanofluid variation as a function of nanoparticle ratio and MD simulation time. (b) The stability time of defined nanofluid as a function of initial temperature.

the absorption force from atomic channel inside MD simulation box. Inserting this attraction force into the simulated nanofluid restricted the atomic evolution of H_2O-fullerene nanofluid particles in the vicinity of atomic walls. Furthermore, atomic evolution of defined compounds inside MD box affected by nanoparticles aggregation process and should be condidered in actual cases. Atomic representaionao of aggragation process depicted in figure 11.

The velocity profile of H_2O-fullerene nanofluid as a function of nanoparticle atomic ratio depicted in figure 12 (a). Computationally, this atomic parameter indicated the time evolution of H_2O-fullerene nanofluid particles in MD box. Our results show that nanofluid particles velocity converged to maximum ratio in the middle union of simulation box. Furthermore, this parameter converged a minimum value in the initial and final bins. Numerically, the maximum velocity of H_2O-fullerene nanofluid particles changes from 0.013 $\AA$/ps to 0.004 $\AA$/ps by nanoparticles ratio varies from 1% to 10%, respectively. Also, temperature profile of simulated nanofluid particles has similar manner, as shown in figure 12 (b). This physical profile converged the maximum value in the middle union of simulation box and reached to a minimum value in initial and final bins. The numerical ratio of this physical parameter listed in Table 4. The results obtained from this part of the study show that the atomic mobility of simulated nanofluid reach to maximum value by 4% nanoparticle adding to base-fluid which this calculation show the best thermal behavior of H_2O-fullerene nanofluid by 4% fullerene inserting to pristine base-fluid.

The thermoelectric effect is another important phenomenon, occurring in atomic structures by the atoms' temperature fluctuations inside MD box. Physically, the thermoelectric effect is the direct conversion of temperature differences to electric voltage and vice versa via a thermocouple [52]. By using MD simulations, the atoms' evolution and so atomic charge displacement in the modeled compounds can be estimated. In LAMMPS package these evolutions in the defined structures was estimated by using DUMP output. In final section of this computational work, we reported the thermoelectric phenomenon after t= 10 ns. Figure 13 (a), indicated the electric voltage changes of simulated nanofluids as a function of the initial temperature. MD simulation results indicated by temperature increasing, total voltage can be detected inside box by adding fullerene nanoparticles to pristine fluid. Numerically, electric voltage which created in atomic compounds varioes from 33.11 V to 40.22 V value by adding nanoparticles with 4% atomic ratio. This phenomenon in atomic structures arises from the effective charge existence in individual atoms. So, time evolution and positions' changes of these atoms cause effective voltage creation by the temperature/atoms fluctuations changes. Thermal stability of simulated nanofluid can be restricted actual applications of them. In the final section of current research, temperature of H_2O-fullerene nanofluid set at 300, 350, 400, and 500 ^oC, and simulation time which needed to atomic compound get unstable reported. MD outputs indicated by temperature increasing inside simulation box, the stability time of the total structure decreases to 57.31 ns (see figure 13 (b)). This thermal result arrised from atomic fluctuations amplitude increasing by temperature enlarging and attraction force decreasing between various atoms.

Table 4. The maximum value of density/velocity/temperature profile and effective voltage of H_2O-fullerene nanofluid in MD simulation box (after t= 10 ns).

Atomic Ratio of Fullerene Nanoparticles (%)	Maximum Density (atom/$Å^3$)	Maximum Velocity $Å$/ps	Maximum Temperature ^{o}C	Effective Voltage (V)
1	0.019	0.013	452.19	33.11
2	0.023	0.011	401.39	35.28
3	0.027	0.008	388.24	38.01
4	0.029	0.005	321.36	40.22
10	0.032	0.004	315.15	39.03

4. Conclusion

Current Molecular Dynamics (MD) simulations described the effect of Fullerene and doped fullerene nanoparticles on the atomic/thermal evolution of Water base-fluid. Fullerenes nanoparticles were added to base-fluid by 1% to 10% atomic ratios. Technically, the Universal Force Field (UFF) and TERSOFF are appropriate interatomic potentials to describe the atomic and thermal evolution of water-fullerene nanofluid and hybrid nanofluid. The total energy of simulated nanofluids changes from -389.36 eV to -725.06 eV by fullerene nanoparticles atomic ratio changes from 1% to 10%, respectively. The MD outputs indicated that fullerene nanoparticles implementing to base-fluid with 4% atomic ratio would improve the thermal behavior of nanofluid appreciably. So, fullerene/water nanofluid was used as the heat transfer fluid to enhance the energy efficiency of the nuclearl heat exchangers.
Also, coolants could be replaced by hybrid-nanofluids. Our results show that thermal-conductivity in hybridnanofluid increases up to 20% and heat transfer performance improve. Numerically, thermal conductivity of water-fullerene nanofluid was increased to 0.82 W/m.K. Heat flux of the modeled structure reached to 2019 KW/m^2 after t= 10 ns. By 4% fullerene adding to water base-fluid, the aggregation time of fullerene nanoparticles converged to 5.84 ns. Also, the effective voltage was detected in simulated nanofluid after t= 10 ns. Numerically, this parameter ratio reached to 40.22 V by using 4% fullerene nanoparticles inside base-fluid. Furthermore, density, velocity, and temperature profile of water-Fullerene nanofluid have affected by fullerene atomic ratio. Numerically, the maximum value of these profiles have reached to 0.029 atom/$Å^3$, 0.005 $Å$/ps, and 321 ^{o}C by a nanoparticle atomic ratio increase to 4%. This MD simulation has been performed at high temperature for the nuclear industry applications for the first time. Thermal power of nanofluid/hybridnanofluid can be improved by fullerenes ratio optimization inside the MD box. Numerically, by the temperature increase of nanofluid/hybridnanofluid structure to 625.15 K, thermal power of nanofluid/hybridnanofluid reache to 3881 MW/3988 after t= 10 ns. The thermal efficiency can be increased by more than 30% by adding concentration of nanoparticles as low as 1–4 vol%.

Conflict of interest statement:

The authors declare that they have no conflict of interest.

References

[1] K. E. Drexler. *Engines of Creation: The Coming Era of Nanotechnology*. Doubleday, 1th edition, 1986.

[2] K. E. Drexler. *Nanosystems: Molecular Machinery, Manufacturing, and Computation*. New York: John Wiley and Sons, 1th edition, 1992.

[3] A. W. Hübler and O. Osuagwu. *Complexity*, **15**:48, 2010.

[4] E. Shinn, A. Hübler, D. Lyon, M. G. Perdekamp, A. Bezryadin, and A. Belkin. *Complexity*, **18**:24, 2013.

[5] R. Taylor, S. Coulombea, T. Otanicar, P. Phelan, A. Gunawan, W. Lv, G. Rosengarten, R. Prasher, and H. Tyagi. *Journal of Applied Physics*, **113**:011301, 2013.

[6] J. Buongiorno. *ASME Journal of Heat and Mass Transfer*, **128**:240, 2006.

[7] W. J. Minkowycz, E. Sparrow, and J. P. Abraham. *Nanoparticle Heat Transfer and Fluid Flow*. CRC Press, 1th edition, 2012.

[8] S. K. Das, S. U. S. Choi, W. Yu, and T. Pradeep. *Nanofluids: Science and Technology*. Wiley-Interscience, 1th edition, 2007.

[9] H. Chen, S. Witharana, Y. Jin, C. Kim, and Y. Ding. *Particuology*, **7**:151, 2009.

[10] D. M. Forrester, J. Huang, V. J. Pinfield, and F. Luppé. *Nanoscale*, **8**:5497, 2016.

[11] L. Yang, W. Ji, M. Mao, and J. Huang. *Journal of Cleaner Production*, **257**:120408, 2020.

[12] R. Bakhtiari, B. Kamkari, M. Afrand, and A. Abdollahi. *Powder Technology*, **385**:466, 2021.

[13] Z. Xuan, Y. Zhai, M. Ma, Y. Li, and H. Wang. *Journal of Molecular Liquids*, **323**:114889, 2021.

[14] H. Eshgarf, R. Kalbasi, A. Maleki, M. S. Shadloo, and A. karimipour. *Journal of Thermal Analysis and Calorimetry*, **144**:1959, 2021.

[15] S. Ahmad, W. Deng, H. Liu, S. A. Khan, J. Chen, and J. Zhao. *Applied Thermal Engineering*, **195**:117183, 2021.

[16] J. D. Bernal. *The Bakerian Lecture, 1962 The structure of liquids*. Royal Society of London. Series A, 1964.

[17] B. J. Alder and T. E. Wainwright. *Journal of Chemical Physics*, **31**:459, 1959.

[18] A. Rahman. *Physical review*, **136**:A405, 1964.

[19] N. A. Jolfaei, N. A. Jolfaei, M. Hekmatifar, A. Piranfar, D. Toghraieand R. Sabetvand, and S. Rostami. *Computer Methods and Programs in Biomedicine*, **185**:105169, 2020.

[20] A. Asgari, Q. Nguyen, A. Karimipour, Q. Bach, M. Hekmatifar, and R. Sabetvand. *International Journal of Thermophysics*, **41**:126, 2020.

[21] A. Z. Ashkezari, N. A. Jolfaei, M. Hekmatifar, D. Toghraie, R. Sabetvand, and S. Rostami. *Computer Methods and Programs in Biomedicine*, **188**:105256, 2020.

[22] W. M. Brown, P. Wang, S. J. Plimpton, and A. N. Tharrington. *Computer Physics Communications*, **182**:898, 2011.

[23] W. M. Brown, A. Kohlmeyer, S. J. Plimpton, and A. N. Tharrington. *Computer Physics Communications*, **183**:449, 2012.

[24] S. Plimpton. *Journal of Computational Physics*, **117**:1, 1995.

[25] W. L. Jorgensen, J. Chandrasekhar, J. D. Madura, R. W. Impey, and M. L. Klein. *The Journal of Chemical Physics*, **79**:926, 1983.

[26] A. K. Rappe, C. J. Casewit, K. S. Colwell, W. A. Goddard, and W. M. Skiff. *Journal of the American Chemical Society*, **114**:10024, 1992.

[27] J. E. Lennard-Jones. *Proceedings of the Physical Society*, **43**:461, 1931.

[28] J. Tersoff. *Physical review B*, **37**:6991, 1988.

[29] D. W. Brenner. *Physica Status Solidi B.*, **217**:23, 2000.

[30] D. C. Rapaport. *The Art of Molecular Dynamics Simulation*. DCR Rapaport, 2th edition, 2004.

[31] S. Nosé. *Journal of Chemical Physics*, **81**:511, 1984.

[32] G. William. *Physical Review A*, **31**:1695, 1985.

[33] L. Verlet. *Physical Review*, **159**:98, 1967.

[34] W. H. Press, S. A. Teukolsky, W. T. Vetterling, and B. P. Flannery. *Numerical recipes 3rd edition: The art of scientific computing*. Cambridge University Press, 1th edition, 2007.

[35] D. Baraff and A. Witkin. *The 25th International Conference on Computer Graphics and Interactive Techniques*, :43, 1998.

[36] H. Ernst, Ch. Lubich, and W. Gerhard. *Acta Numerica*, **12**:399, 2003.

[37] H. Jin, T. Andritsch, I. A. Tsekmes, and R. Kochetovand P. H. F. Morshuisand J. J. Smit. *IEEE Conference on Electrical Insulation and Dielectric Phenomena*, :711, 2013.

[38] M. Hestenes, R. Magnus, and E. Stiefel. *Journal of Research of the National Bureau of Standards*, **49**:409, 1952.

[39] T. A. Straeter. *NASA Technical Reports Server*, :1, 1971.

[40] J. Dunkel and S. Hilbert. *Physica A: Statistical Mechanics and its Applications*, **370**:390, 2006.

[41] D. C. Rapaport. *The Art of Molecular Dynamics Simulation*. Cambridge University Press, 1th edition, 2004.

[42] G. N. I. Clark, C. D. Cappa, J. D. Smith, and R. J. Saykally. *Molecular Physics*, **108**:1415, 1996.

[43] P. Ball. *Nature*, **452**:291, 2008.

[44] M. S. Green. *Journal of Chemical Physics*, **22**:398, 1954.

[45] R. Kubo. *Journal of the Physical Society of Japan*, **12**:570, 1957.

[46] B. Reding and M. Khayet. *Scientific Reports*, **12**:9603, 2022.

[47] Z. Liu and Z. Q. Zhang. *AIP Advances*, **7**:125208, 2017.

[48] H. Zou, C. Chen, M. Zha, K. Zhou, R. Xiao, Y. Feng, L. Qiu, X. Zhang, and Zh. Wang. *Journal of Thermal Science*, **30**:1908, 2021.

[49] Ch. Goupil, H. Ouerdane, K. Zabrocki, W. Seifert, N. F. Hinsche, and E. Müller. *Continuum Theory and Modeling of Thermoelectric Elements*. Wiley, 1th edition, 2016.

[50] 14.BU.1 0.Y.TM.PZ.PRR032 Experimental verification. *Reactor plant V-446. Explanatory report. Part 4*. OKB Gidropress, 1th edition, 2000.

[51] 14. BU.10.Y.TM.PZ.PRR041 Description of design conditions. *Reactor plant V-446. Explanatory report. Part 2*. OKB Gidropress, 1th edition, 2000.

[52] Shi. Yunhong, A. Awatef, Kh. Yacine, Zh. Long, M. Sharifpur, and G. Cheraghian. *Journal of Molecular Liquids*, **346**:117093, 2022.